Soft Switching Condition Analysis for a Novel ZVS-SVM Controlled Three-Phase Boost PFC Converter

Rui Li , Dehong Xu, Bo Feng
Institute of Power Electronics
Zhejiang University
Hangzhou, P. R. China 310027
liruiqd@zju.edu.cn

Kazuaki Mino， Hidetoshi Umida
Fuji Electric Advanced Technology Co., Ltd.
Tokyo 191-8502 Japan

***Abstract*- The ZVS-SVM controlled three-phase boost rectifier proposed by the authors can realize ZVS operation for all switching devices. In addition, the anti-parallel diode reverse recovery of all switch devices' is well suppressed. Moreover, SVM can be realized with switch devices operating at the fixed switching frequency. In this paper, the soft switching condition of the ZVS-SVM controlled three-phase boost PFC is analyzed. The relationship between the switches' voltage stress and circuit parameters is studied. The relationship between the circuit parameters and the soft switching condition is also investigated. The results is verified by a 3kW prototype.**

I. INTRODUCTION

The six-switch three-phase boost rectifier is a preferred topology with several advantages such as lower current stress, high efficiency, and small input EMI filter for higher power application. However the anti-parallel diodes of all the switches in the rectifier experience reverse recovery process which will cause severe switching loss, high di/dt and EMI problems.

For passing years, many works about soft switching for three-phase rectifier or inverter have been undertaken to solve the diode reverse recovery problem. The DC-rail ZVT boost rectifier proposed in [1] can realize the ZVS of the main switches. However the auxiliary switch is in hard switching. The auxiliary resonant commutated pole (ARCP) converter can reduce the auxiliary circuit conduction loss. However it needs six extra auxiliary switches [2]. The resonant dc link (RDCL) proposed in [3, 4] has the simplified topology. However the voltage stress in switches of RDCL converter is higher. The active clamped RDCL in [4, 6] has a low voltage stress. However, RDCL and ACRDCL converters have to use discrete pulse modulation (DPM), which normally causes undesirable sub-harmonics [5].

The ZVS-SVM controlled three-phase boost rectifier proposed by the authors [8, 9]. It has a low voltage stress in both main switches and auxiliary switch. The switch anti-parallel diodes' reverse recovery is suppressed well and all the switches can be turned on under zero voltage condition. Moreover, both the main switches and the auxiliary switch has the same and fixed switching frequency.

In this paper, the soft switching condition of the ZVS-SVM controlled three-phase boost PFC is analyzed. How the switches' voltage stress is influenced by circuit parameters is studied. The relationship between the circuit parameters and the soft switching condition is also investigated. A 3kW DSP (TMS320F2407A) controlled boost rectifier prototype is built to verify the theory.

II. OPERATION PRINCIPLE OF THE ZVS-SVM CONTROLLED BOOST RECTIFIER

A. Converter topology and Modulation scheme

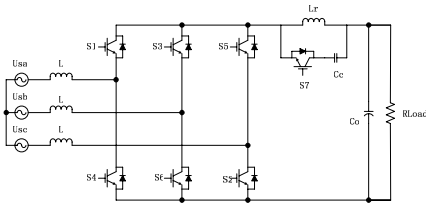

Fig.1. ZVS-SVM controlled active-clamp three-phase boost rectifier

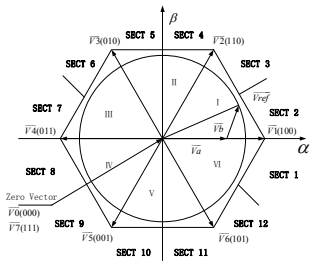

(a) voltage space vectors

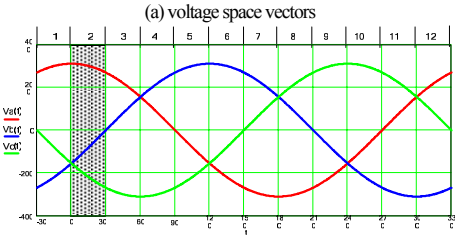

(b) Three-phase voltages

Fig. 2. Three-phase voltages and voltage space vectors

Fig.1 shows the topology of the ZVS-SVM controlled three-phase boost PFC. This topology consists of a standard PWM rectifier and a clamp branch. The clamp branch consists of an active switch, a resonant inductor Lr and a clamping capacitor Cr. Although the

topology is the same as that of ACRDCL converter, the control pattern is quite different. A zero voltage switching space vector modulation (ZVS-SVM) control is used.

In the ZVS-SVM control, the phase voltage's waveform and voltage vector's definition are shown in Fig. 2. The whole utility cycle is divided into 12 sectors. Since the operation of the converter is symmetrical in every 30^o, we assume that the converter is operating in sector 2 where Ia>0 and Ic<Ib<0. In this sector, phase A has the highest voltage and input current, then switch S1 is always conducting, while the switches in the other two phases are controlled in the PWM manner. There are three switch states in one switching cycle, as shown in Fig. 3. The three switch states are state 100, state 111 and state 110. The equivalent circuits of these three states are shown in Fig. 4.

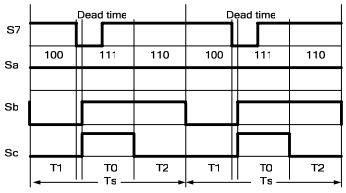

Fig. 3 switching sequence in sector 2: 100-111-110-100

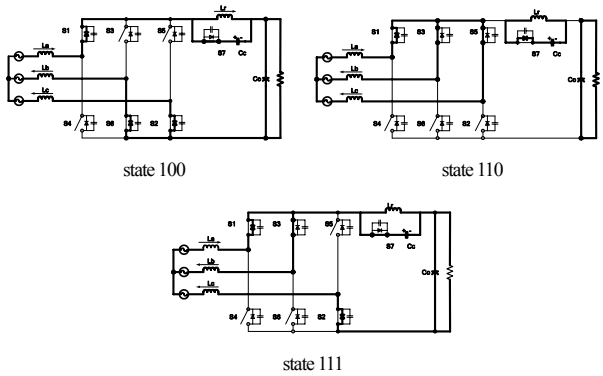

Fig. 4 operation stages of three switching states

B. Zero voltage switching of the switches

Under the ZVS-SVM scheme, when switching state 100 is to be changed to state 111, the switch S3 and S5 are to be turned on simultaneously. Before this instant, the auxiliary switch S7 is turned off. Thus the energy in the resonant inductor Lr will discharge the parallel capacitor of the switch S3, S4, and S5, making the bridge voltage resonant to zero. S3 and S5 can be ZVS turned on. And Lr can suppress the reverse recovery current of switch S2's and S6's anti-parallel diodes. When the switch anti-parallel diode finish the reverse recovery, the current of the resonant inductor flow through anti-parallel diode of the auxiliary switch S7. So the auxiliary switch S7 is always turned on under ZVS. S7 is conducting during most of the time in one switching cycle. In the state change from 111 to 110, the current change from S5 to S2's anti-parallel diode. In the state change from 110 to 100, the current change from S3 to S6's anti-parallel diode. These two transitions are normal soft-switching.

III. Analysis Of The Soft Switching Condition Of The SVM Controlled Boost Rectifier

A. Operation stage analysis of the soft switching rectifier

Since in the ZVS-SVM control, the operation of the conveter is symmetrical in every 30^o, sector 2 where Ia>0 and Ic<Ib<0 (0°~30°) is still taken as an example to analyze. Following assumptions are made to simplify the analysis of the proposed PFC converter:

The capacitances C1 to C6 paralleled with switches S1 to S7 respectively include parasitic capacitances and external capacitances. The input filter inductor L1, L2, L3 is so large that their current can be considered as constant current source in one switching cycle. The output filter capacitor Co is represented by a constant voltage source. The value of active clamping capacitor Cc is large enough so that the voltage can be seen as a constant. The resonant frequency of Cc and Lr is much lower than the operation frequency of the converter.

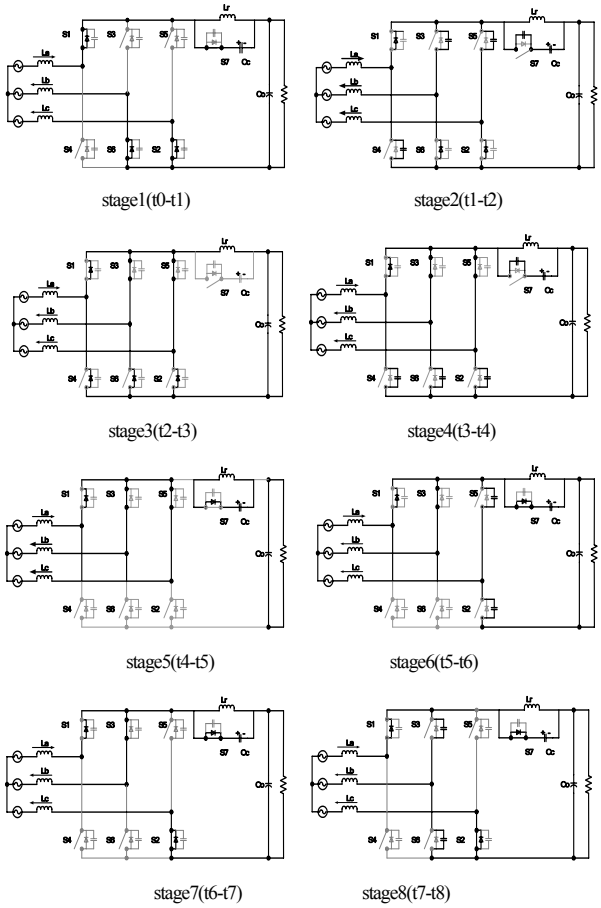

Fig. 5 operation stages of ZVS PFC

The operation stage and key waveforms of the ZVS three-phase PFC are shown in Fig.5 and Fig.6 respectively. The switching cycle can be divided into 8 stages.

Stage1(t0-t1): In this stage, S1,S2,S6 and the auxiliary switch S7 is conducting. The current in resonant inductor Lr increases at the rate of: $di_{Lr}/dt = V_{Cc}/Lr$.

Stage2 (t_1-t_2): The auxiliary switch S7 is turned off in t1, the resonant inductor Lr will discharge the main switch S3,S4,S5's paralleling capacitors C3,C4,C5 . At time t2, the voltages on these capacitors decreases to zero and the anti-parallel diode of these main switches start to conduct. The main switch S3 and S5 are turn on with zero voltage switching. At time t2 the voltage on S7 reaches $Vo+V_{Cc}$.

Stage3 (t2-t3): From this stage, the anti-parallel diode of S6 and S2 experience diode reverse recovery. Due to the existence of the resonant inductor Lr, the diode reverse recovery is suppressed. At time t3, the current of the anti-parallel diodes of both switch S6 and S2 drop to zero. The current in resonant inductor Lr changes at the rate of: $di_{Lr}/dt = -V_o/Lr$.

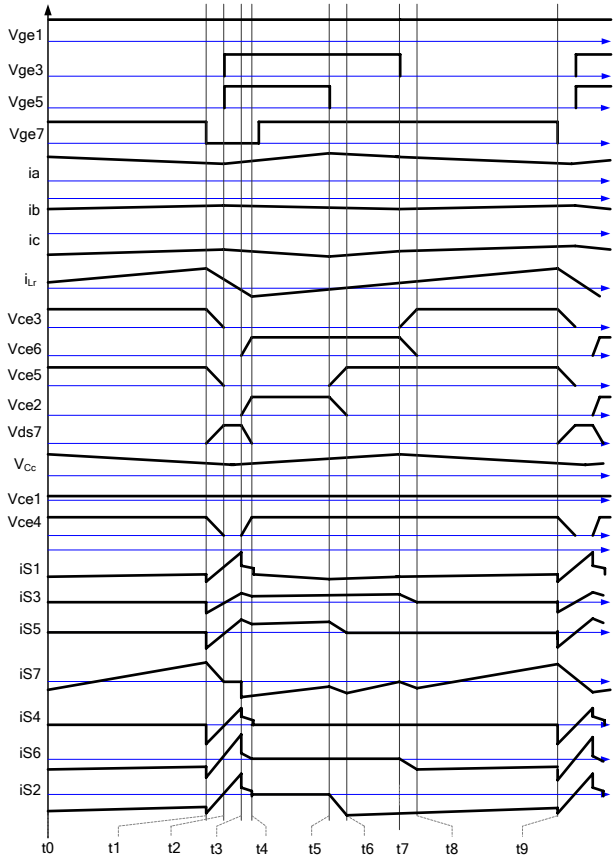

Fig. 6 steady-state waveforms of the proposed converter

Stage4 (t3-t4): At t3, the voltage on S6 and S2 start to rise, Lr, C2, C4, C6 and C7 start to resonance. The voltage on S7 starts to decrease. At t3, the voltage on S7 decrease to zero, and the anti-parallel diodes of S7 start to conduct. S7 can be ZVS turn on.

Stage5 (t4-t5):At t4, the diode reverse recovery process completes. The circuit enters the state 111. The main switches S1, S3, S5 and the auxiliary switch S7 are turn on. The resonant inductor Lr is charging the clamping capacitor Cc.

Stage6 (t5-t6):At t5, the main switch S5 is turned off. Since the existence of C5 and C2, it is ZVS turn off. The input inductor Lc will charge C5 and discharge C2.

Stage7 (t6-t7):At t6, the voltage on S2 decrease to zero, the anti-parallel diode starts to conduct. S2 can be ZVS turn on. The circuit enters state 110, the last time is decided by the SVM control.

Stage8 (t7-t8):At t7, the main switch S3 is turned off, since the existence of C3 and C6, it is ZVS turn off. The input inductor Lb will charge C3 and discharge C6. At t8, the voltage on S6 decrease to zero, the anti-parallel diode starts to conduct. S6 can be ZVS turn on. The circuit enters start 100. After t8, the next switching cycle starts again.

B. Relationship between the circuit parameters and voltage stress on the switches

According to the stage analysis, the voltage stresses on the switches consist of the active clamping voltage V_{Cc} and the output voltage V_o, for V_o is the constant quantity required by the output load, only V_{Cc} can be influenced by the circuit parameters.

$$V_{Cc} = \frac{2TV_o^2}{2V_oT - 3mL_rI_{in} - 4L_rV_o\sqrt{\frac{3C+C_7}{L_r}}} \quad (1)$$

From the formula (1), it can be seen that the resonant parameters as well as the output voltage and the input current can influence the active clamping voltage stress. The switching frequency can also impact the active clamping voltage stress. For the modulation index m and the input current I_{in} is determined by the input phase voltage V_{in} and the output power P_o, so V_{in} and P_o can influence the active clamping voltage stress too.

The theoretic curves between the active clamping voltage stresses and the circuit parameters are shown in Fig.7.The parameters of the circuit in Fig.7 are: V_{in}=220V, V_o=620V, P_o=3000W, L=12mH, L_r=80uH, C_c=45uF. The operation frequency f=12.8kHz. The parallel capacitors of the switches are $C_1=C_2=\ldots=C_7=2n$F.

Fig.7(a) shows the relationship between the active clamping voltage and the voltage vector angle vector, it can be seen from the fig that V_{Cc} will not change in the whole sector.

Fig.7(b) shows the relationship between V_{Cc} and the resonant inductor L_r, the augment of the L_r will result in the higher of active clamping voltage.

Fig.7(c) shows the relationship between V_{Cc} and the resonant inductor capacitor C_r, the increasing of C_r will make the active clamping voltage higher than before.

Fig.7(d) shows the relationship between V_{Cc} and the operation frequency f, the higher the operation frequency is, the higher the active clamping voltage will be.

Fig.7(e) shows the relationship between V_{Cc} and the output power P_o, the increasing of the output power will make the active clamping voltage higher than before.

The experimental curves between the active clamping voltage stresses and the circuit parameters are also shown in Fig.7.The experimental parameters are same with the parameters shown above. The experimental curve is similar with the theoretic curve. We can see that with appropriate resonant parameter design, the switch voltage stress can be controlled to the value only a little higher than the output DC voltage.

C. Relationship between the circuit parameters and the soft switching

condition

According to the stage analysis explained above, the auxiliary switch always satisfies zero-voltage turn–on condition. The ZVS condition for the main switches lies on if the resonant inductor has enough energy to discharge the paralleling capacitor of the main switches and resonant the bridge voltage to zero. The minimum bridge voltage in the resonant process is:

$$V_{CMIN} = (I_a + \frac{K \cdot V_{CE(on)}}{L_r} \cdot T - \frac{3 \cdot m I_{IN}}{2}) \sqrt{\frac{L_r}{3C + C_7}} \quad (0 < k < 1) \qquad (2)$$

Where $V_{CE(on)}$ is the conduction voltage drop of the auxiliary switch. If V_{CMIN} is less than zero, the ZVS of main switches is achieved. It can be seen from the formula that not only the circuit resonant inductor, but also the input current I_{in} and $V_{CE(on)}$ can influence the soft switching condition. For the modulation index m and the input current I_{in} is determined by the input phase voltage V_{in} and the output power P_o, so V_{in} and P_o can influence the soft switching condition too.

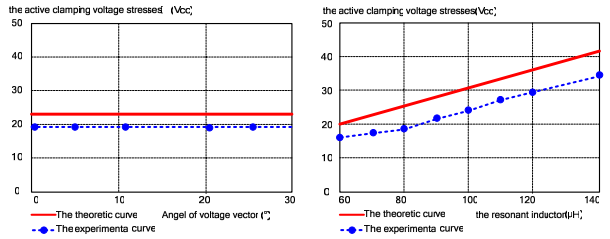

(a) active clamping voltage stresses vs. θ (b) active clamping stresses vs. L_r

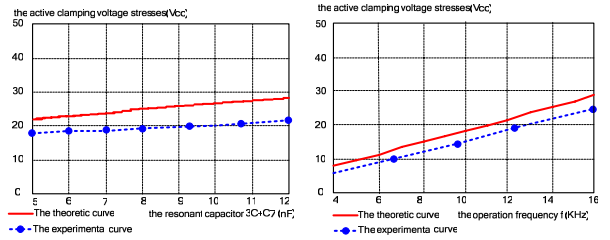

(c) active clamping stresses vs. C_r (d) active clamping stresses vs. f

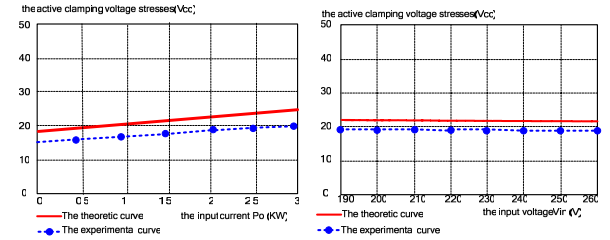

(e) active clamping stresses vs. P_o (f) active clamping stresses vs. V_{in}

Fig.7 Curve between the active clamping voltage stresses on the switches and the circuit parameters

When choose the resonant inductor parameter as 21uH, but do not change other parameters, the curve of the space vector angle vs. V_{CMIN} can be gained, which is shown in Fig.8. Fig.8 shows that the space vector angle can also affect the soft switching realization. If the space vector angle is larger than 25° in fig.8, V_{CMIN} is zero, then the soft switching of main switches is achieved. If the space vector angle is smaller than 25° in fig.8, V_{CMIN} is larger than zero, the soft switching of main switches can not be achieved.

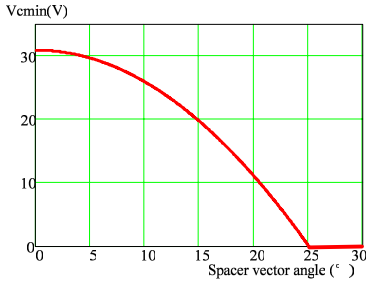

Fig.8 the vector angle in sector 2 vs. V_{CMIN}

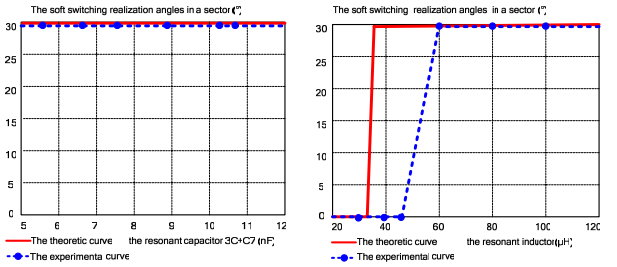

(a) soft switching realization angles vs. Cr (b) soft switching realization angles vs. Lr

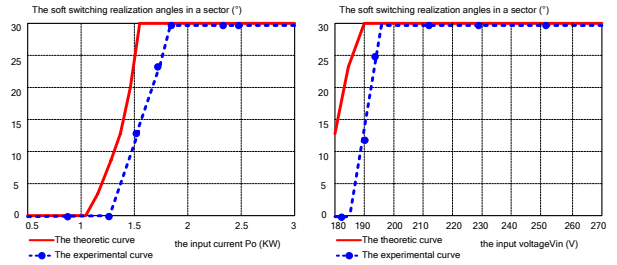

(c) soft switching realization angles vs. P_o (d) soft switching realization angles vs. V_{in}

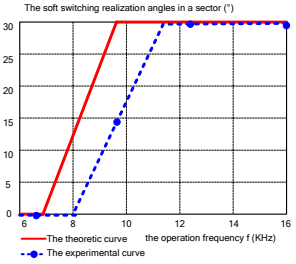

(e) soft switching realization angles vs. f

Fig.9 Curve between the circuit parameters and how many angles of absolute soft witching can be realized in one sector of 30°

If the switches of the PFC converter can achieve the soft switching condition in the whole voltage space vestor, the converter will have a higher efficiency. So it is important to analyze the influence of the circuit parameters to the soft switching realization.

Since the operation of the conveter is symmetrical in every 30°, sector 2 where Ia>0 and Ic<Ib<0 (0°~30°) is still taken as an example to analyze. The theoretic curve between the circuit parameters and how many angles of absolute soft switching can be realized in a voltage sector 2 are shown in Fig.9. The calculation parameters of the circuit are same to above.

Fig.9(a) shows the relationship between the soft switching realization angles and the resonant capacitor Cr. Because the alter of circuit resonant capacitor's parameter can not change the polarity of V_{CMIN}, which can be seen in the formula 2,the resonant capacitor can not determine if the soft switching can be realized. While in the formula 2, the absolute value of V_{CMIN} can be affected by Cr, so adjusting of the resonant capacitor's parameter can still influence the soft switching realization.

Fig.9(b) shows the relationship between the soft switching realization angles and the resonant inductor Lr. The more the increasing of the parameters of resonant inductance, the easier the soft switching be achieved.

Fig.9(c) shows the relationship between the soft switching realization angles and the output power P_o, the soft switching will be realized easily if the output power P_o is higher.

Fig.9(d) shows the relationship between the soft switching realization angles and the input phase voltage, according to this fig, increasing the input phase voltage will help the realization of the soft switching.

Fig.9(e) shows the relationship between the soft switching realization angles and the converter's operation frequency. The higher the operation frequency is, the easier the soft switching condition can be realized.

The experimental curves between the circuit parameters and how many angles of absolute soft switching can be realized in voltage space vector 2 are also shown in Fig.9. The experimental parameters are same with the parameters mentioned above. The experimental curve is similar to the theoretic curve, because of the existence of circuit resistance, the soft switching realization is a little more difficult than the theoretics analysis. With appropriate circuit parameters, it is easy to achieve soft switching in the ZVS-SVM scheme.

IV. Experimental Results

A 3 kW prototype of the ZVS-SVM controlled boost rectifier, as shown in Fig. 1, is built to verify the theory. It is controlled by DSP (TMS320F2407A). The parameters of the circuit have been mentioned above. The main switches, S1~S6: IRGPH50K. The auxiliary switch S7: CT60AM-20F. The CE voltage and the driving signal of the main switch and the auxiliary switch is shown in Fig. 10 and Fig. 11 respectively. As can be seen that the CE voltage drop to zero before the driving signal turn high. Thus both the main switch and auxiliary switch is ZVS turn on. The input voltage and current is shown in Fig.12. The clamping voltage is less than 40V, as shown in Fig.13. Thus the voltage stress of the switches in the proposed rectifier is low.

V. Conclusion

The soft switching condition of the ZVS-SVM controlled three-phase boost PFC is analyzed. The maximum switch voltage stress can be influenced by the resonant parameters and the input current. The resonant parameters and the input current can also affect the realization of soft switching. With appropriate circuit parameters, it is easy to achieve soft switching in the ZVS-SVM scheme and the maximum switch voltage stress are only a little higher than the output voltage. It is suitable for high density rectifier application.

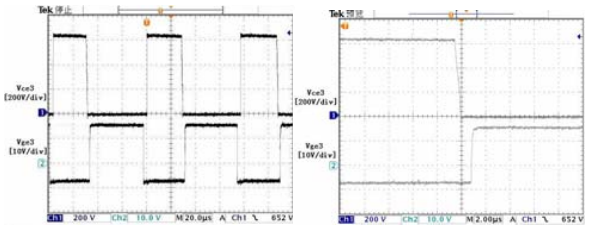

(a) time 20us/div (b) time 2us/div

Fig. 10 CE voltage and driving signal on main switch

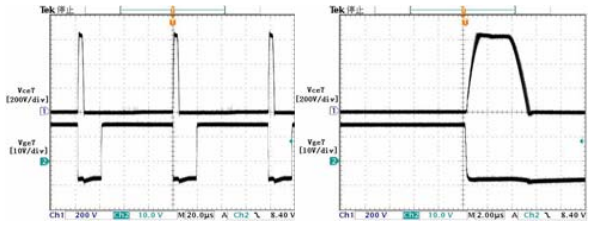

(a) time 20us/div (b) time 2us/div

Fig.11 CE voltage and driving signal on auxiliary switch

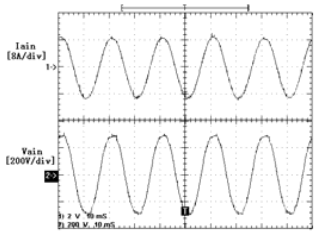

time 10ms/div

Fig. 12 Input voltage and current

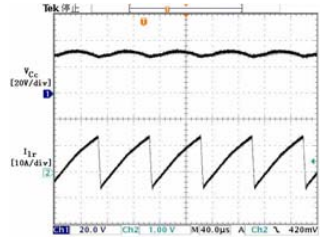

time 40us/div

Fig. 13 Current of Lr and voltage on clamping capacitor

Acknowledgment

The author would like to thank the support of Fuji Electric Advanced Technology Co. Ltd.

REFERENCES

[1] Y. Jiang, H. Mao, F. C. Lee and D. Borojevic, "Simple high performance three-phase boost rectifiers," IEEE Proc. of PESC' 94, 25th Annual IEEE 20-25, June, 1994, pp.1158-1163

[2] R.W. De Doncker and J.P. Lyons, "The auxiliary commutated resonant pole converter" Proc. of IAS'90. Conference Record of the 1990 IEEE 7-12 Oct. 1990 pp.1228-1235.

[3] D. M. Divan, "The resonant dc-link converter- a new concept in power conversion" IEEE trans on Industrial Applications, Volume 25, Issue 2, March-April 1989 Page(s):317 – 325

[4] D. M. Divan, and G. Skibinski, "Zero-switching-loss inverters for high power applications," IEEE trans on Industrial Applications, Volume 25, Issue 4, July-Aug. 1989 Page(s):634 - 643

[5] G. Venkataramanan, D. M. Divan and T. Jahns, "Discrete pulse modulation strategies for high frequency inverter system" Power Electronics, IEEE trans on Volume 8, Issue 3, July 1993 Page(s):279 – 287

[6] M. Nakaok, H.Yonemori, and K. Yurugi, "Zero-Voltage soft-switched PDM three phase AC-DC active power converter operating at unity power factor and sinewave line current" Proc. of PESC'93, 24th Annual IEEE 20-24 June 1993 pp. 787-794

[7] H. Mao, F. C. Lee, D. Boroyevich, S. Hiti, " Review of High-performance Three-phase power-factor correction circuits" IEEE trans on Industrial electronics, Vol 44, NO.4 Aug, 1997, pp.437446.

[8] D. Xu, B. Feng, " Novel ZVS Three-Phase PFC Converters and Zero-Voltage-Switching Space Vector Modulation" IEEE Proc. of PESA'04, 2004 First International Conference on 9-11 Nov. 2004 ,pp. 222 – 229

[9] B. Feng, D. Xu, W. Wang, J. Xu, " A Novel Zero Voltage Switching SVM (ZVS-SVM) Controlled three phase boost rectifier" Proc. of APEC'05, Twentieth Annual IEEE Volume 1, 6-10 March 2005, pp. 642-647